Sādhanā (2025) 50:102
https://doi.org/10.1007/s12046-025-02748-4

Frequency-independent antennas for low-frequency radio telescope

AGARAM RAGHUNATHAN[1,*], K KAVITHA[1], SATHISH KEERTHIPRIYA[1], S ARASI[1], H N NAGARAJ[1] and SHIV K. SETHI[2]

[1]Electronics Engineering Group, Raman Research Institute, Bangalore, India
[2]Astronomy and Astrophysics Group, Raman Research Institute, Bangalore, India
e-mail: raghu@rri.res.in; kavi10ece@gmail.com; keerthi@rri.res.in; arasi@rri.res.in; nraj@rri.res.in; sethi@rri.res.in

MS received 5 February 2024; revised 17 October 2024; accepted 3 February 2025

Abstract. Exploring the universe at low frequencies for sensitive and broadband polarization studies of a range of radio sources is expected to open up a new dimension to radio astronomical observation. Building a low-frequency radio telescope (LFRT) to operate over the frequency band of 30–360 MHz with a wide field-of-view (FOV) capability and an instantaneous bandwidth of 300 MHz is considered most rewarding for observing the low-frequency universe. For this telescope, two reflector-based dipole antennas have been designed with 1:3 bandwidth to operate in the frequency bands of 30–90 MHz and 120–360 MHz to simultaneously cover the frequency band of 30–360 MHz. They are planar, profiled, and tilted to achieve larger bandwidth and frequency-independent radiation and impedance characteristics. The frequency-independent characteristic is expected to ease the calibration of the antenna bandpass response. The antennas have i) a moderate reflection coefficient of less than −4 dB over their operating bands with a smooth spectral response and ii) frequency-independent E-plane radiation patterns having a maximum dispersion in their half-power beamwidths of less than 10% across their operating bands. The structural parameters of the antennas have been optimized using electromagnetic modeling, and the designs have been validated by constructing prototypes.

Keywords. Dipole antenna; Antenna measurements; Radio astronomy.

1. Introduction

Designing antennas with simple geometrical structures and a bandwidth greater than an octave with i) frequency-independent radiation and impedance characteristics, ii) good impedance match, and iii) smooth spectral response is a great engineering challenge. Achieving a larger bandwidth with the desired spectral characteristics requires a clear understanding of the effect of the structural parameters on the electromagnetic properties of the antenna. With this knowledge, electromagnetic modeling of the structure will be carried out and the dimensions will be varied iteratively until the desired response is achieved experimentally.

The scientific motivation for designing a wideband antenna for the low-frequency radio telescope (LFRT) is to probe the sky, which remains almost unexplored at longer wavelengths for a variety of radio astronomical investigations such as detection of transients, measurement of broadband polarization, both steady and transient, of a wide variety of sources including pulsars, study of diffuse non-thermal recombination lines, and high redshift universe [1]. The frequency window of 30–360 MHz is considered as the primary window for these studies, and an antenna capable of operating in this window with a large collecting area and a wide field of view (FOV) is highly desired in radio astronomy.

Several attempts are being made across the globe to design a single antenna element having a decade or more bandwidth with the desired spectral characteristics for observing the sky. However, till date this has been possible using two antennas rather than just one. In the low-frequency array (LOFAR) radio telescope, the operating band of 10–240 MHz has been covered using two antennas: low-band antenna (LBA) [2] for the frequency range of 30–80 MHz and high-band antenna (HBA) [3] for the frequency range of 120–240 MHz. The long wavelength array (LWA) radio telescope [4] uses dipole-type antennas, which can be tuned anywhere between 10 MHz and 88 MHz. The impedance bandwidth of that antenna, under tuned conditions, is much less than the 1:9 bandwidth. The Murchison widefield array (MWA) radio telescope [5] is one of the wide-band low frequency radio telescopes designed specifically to observe the high redshift Universe. It is designed to operate in the frequency range of 80–300 MHz. It uses an active bow-tie antenna as a sensor to observe the sky. SKA-Low is the low frequency radio telescope of

*For correspondence
Published online: 17 May 2025

square kilometer array (SKA) [6] being built to explore the Universe at a wide range of frequencies starting from 50 to 350 MHz. In this telescope, a log-periodic dipole antenna containing multiple resonating elements has been used to cover the entire band.

With the aim of designing an antenna with the largest possible bandwidth, antennas with different smooth profiles were considered for investigation and simulated for their electromagnetic performance. The planar sinusoidally profiled reflector-based dipole antenna designed by us for the detection of epoch of recombination signal [7] in the frequency range of 2–4 GHz was considered as a potential candidate for reoptimizing the structural parameters to achieve larger bandwidth by compromising on the magnitude of the reflection coefficient and dispersion in the half-power beamwidth of radiation patterns across the operating band.

The present design has several important features over existing solutions in terms of i) operating bandwidth, ii) smooth spectral response in the reflection coefficient characteristics, and iii) frequency-independent radiation patterns. The antenna designed is reflector-based and belongs to the class of wire antennas. The antenna structure in the cited reference is modified to achieve a larger bandwidth as high as 1:3. The modification involved sinusoidal profiling the dipole arm for impedance matching and making the arm length short to simultaneously achieve frequency-independent patterns. The thickness of the arm was optimized to have the minimum gain in the direction of horizon so that the antenna is less sensitive to man-made interference. The main challenges faced in the design process were mainly i) obtaining large bandwidth using transmission line balun, ii) achieving reflection coefficient characteristics with modest value and free from spectral features over the larger band, and iii) unacceptable dispersion in the half-power beamwidths of the antenna over the entire frequency range. The problem due to the balun was solved by using a transformer-type balun from Mini-circuits instead of the transmission line balun. The large bandwidth in the reflection coefficient was achieved by optimizing the height of the dipole structure over the reflector. The resulting dispersion in the beamwidths was controlled by tilting the dipole arms optimally. Using the broadband antenna designed, radio sky can be effectively explored over as large bandwidth as 1:10 starting from 30 MHz to 360 MHz. This includes the low-frequency regime spanning over 30–90 MHz, which has remained almost unexplored in detail. Due to the frequency-independent nature of the antenna pattern and its smooth spectral characteristics, bandpass calibration of the antenna can be easily performed in the process of data analysis. Two prototype antennas have been built after appropriate scaling, one in each frequency band of 30–90 MHz and 120–360 MHz, and have been tested for their smoothly varying impedance and frequency-independent radiation characteristics. Some of the results obtained from these antennas are also referred in [8].

On comparing frequency-independent antennas designed by us with the equiangular spiral antennas and log periodic antennas, we observe that the latter are electrically large in structure and have limitations in use in sensitive experiments involving the detection of very faint cosmological signals which have their own characteristic frequency signature. The limitation comes from non-smooth spectral characteristics in both impedance and frequency patterns. This poses a serious challenge in bandpass calibrating the receiver gain across the operating band. Using the antennas developed, sky observation can be performed over 1:10 bandwidth using instead of a single antenna, two antennas. The antennas also have the required electrical performance appropriate for wideband sky observation.

In this paper, section II describes our design objectives motivated by observation of the sky at low frequencies. Our investigations of the effect of structural parameters of the planar sinusoidally profiled reflector-based dipole antenna such as i) height of the antenna above the perfectly conducting reflector, ii) tilt angle of the dipole arms, and iii) design frequency on the performance characteristics are described in section III along with some simulation results. Section IV provides details about the fabrication of prototype dipole antennas. The performance measurements of antennas are described in sections V and VI, and our work is summarized in section VII.

2. Design objectives

The motivation for designing the broadband antenna is in its application of probing the radio sky at longer wavelengths for detecting transients and pulsars over large bandwidth. As this also involves surveying the sky, the antenna is required to have a wide FOV of the order of 2π steradian along with more than an octave bandwidth in the frequency range of 30 to 360 MHz. As the sky is known to be bright at low frequencies, a modest reflection coefficient of about ≤ -4 dB was considered sufficient to couple an adequate amount of sky signal to the receiver system. The bandpass calibration of any broadband device like an antenna is hard if its spectral response has undesired features. Therefore, it is required that the impedance and radiation characteristics of the antenna be frequency-independent or monotonic in nature.

3. Investigation of the effect of structural parameters on the antenna performance

The planar and profiled dipole antenna designed for the detection of the epoch of recombination signal in the frequency range of 2–4 GHz was considered most appropriate for the present investigation of knowing the effect of structural parameters of the antenna on its operating bandwidth, with all the desired electrical properties. Initially, it was aimed at obtaining 1:3 bandwidth so that the band 30–360 MHz could be covered using two antennas, one to cover 30–90 MHz and the second one for 120–360 MHz. The narrow band of 30 MHz in between 90 and 120 MHz was deliberately avoided due to the presence of undesired frequency modulation (FM) band signal. The transmission line-based balun used in the original design was replaced by a transformer-based minicircuit balun TC1-1-13MG2+ for achieving a larger bandwidth.

In the process of investigation, the 2–4 GHz antenna structure was appropriately scaled to operate in the frequency band of 120–360 MHz and its structural and electrical parameters such as i) design frequency, ii) height of the antenna above the perfectly conducting reflector, and iii) tilt of the arms of the dipole antenna were varied one at a time to optimize the antenna performance such as operating bandwidth, radiation patterns, and impedance characteristics in the frequency band of 120–360 MHz. Optimization was carried out by adopting the "variation of parameters" technique in which each of the above parameters was varied over a finite range one at a time. Two electromagnetic simulation software packages WIPL-D [9] and CST Microwave [10] were used during optimization to i) ensure that antenna performance is not constrained by the limitation of either software and ii) cross-verify the performance across two different platforms to gain more confidence, before implementing them.

The design frequency after several iterations of simulation was arrived at 226.5 MHz. The side of the square reflector was set at three wavelengths at the design frequency so that a square array of 5 $\times$ 5 could be implemented on it in future. The height of the dipole antenna was optimized to obtain both a moderate reflection coefficient with smooth variation as a function of frequency and minimum dispersion in the half-power beamwidths of radiation patterns over the entire frequency band. It is observed from figure 1 that a larger distance of the dipole from the reflector results in frequency-independent patterns with a poor reflection coefficient. However, with smaller heights, the reflection coefficient improves, but the radiation patterns will have a large dispersion in their half-power beamwidths. Therefore, after fine-tuning, 284.9 mm was chosen as the optimal height, which resulted in an acceptable value of reflection coefficient (≤ -4 dB). The dispersion observed for this height was improved by tilting each arm of the dipole. The tilt angle was varied from -10 deg to $+10$ deg. The negative sign indicates tilt upward, and the positive sign indicates tilt downward. Its effect on the reflection coefficient and the radiation patterns is shown in figure 2. Tilt of each arm was found to have more influence on the pattern than on the reflection coefficient. Tilt of $+10$ deg of each arm was found to be optimum, which minimized the dispersion resulted while optimizing the antenna height.

This configuration resulted in an included angle of about 160 deg between two arms. The simulated structure of the antenna designed for the frequency range of 120–360 MHz is shown in figure 3. The same structure was scaled by a factor of 4 to obtain the antenna for the frequency range 30–90 MHz as shown in figure 4. Dimensions such as length, dipole thickness, gap between arms, antenna height above the reflector, and the design frequency of both antennas are given in the table 1. The balanced outputs of each of the antennas are passed through TC1-1-13MG2+, which is a transformer-based balun of Mini-circuits, which converts them to single-ended output. The single-ended output is brought down to the antenna base through an air–core coaxial cable.

4. Fabrication details of the antenna

The prototypes of antennas designed are constructed out of a 2-mm-thick aluminum sheet cut to the dimensions as shown in figures 3 and 4. While implementing them, the sinusoidal profile of the antenna was approximated by linear segments for ease of fabrication. A reinforcing framework made of a 10-mm-thick square rod was used to fix the top and bottom sheets of the dipole using M3 screws. The

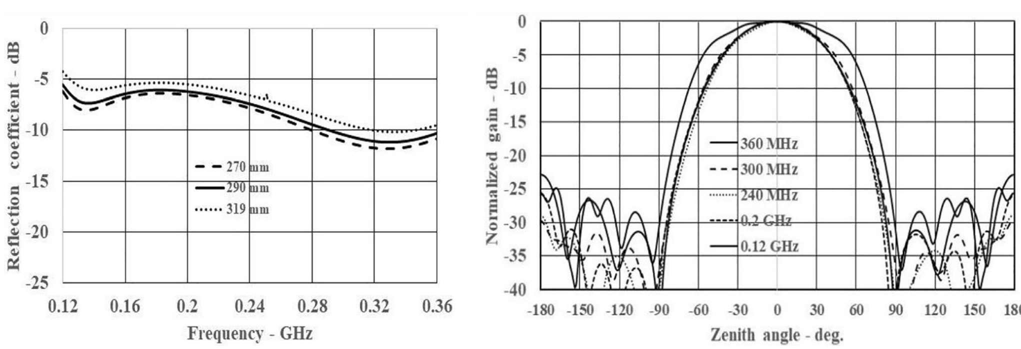

Figure 1. (Left) Effect of antenna height above reflector on the reflection coefficient characteristic and (right) radiation patterns at 120, 200, 240, 300, and 360 MHz.

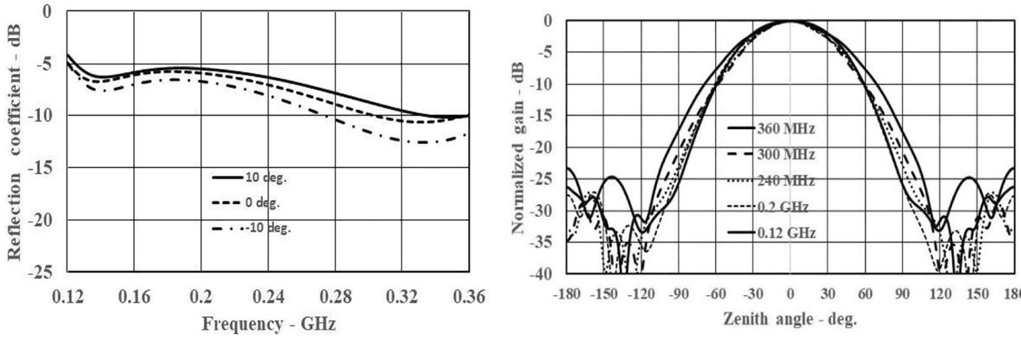

Figure 2. (Left) Effect of tilt of each of the dipole arms on the reflection coefficient characteristic and (right) radiation patterns at 120, 200, 240, 300, and 360 MHz.

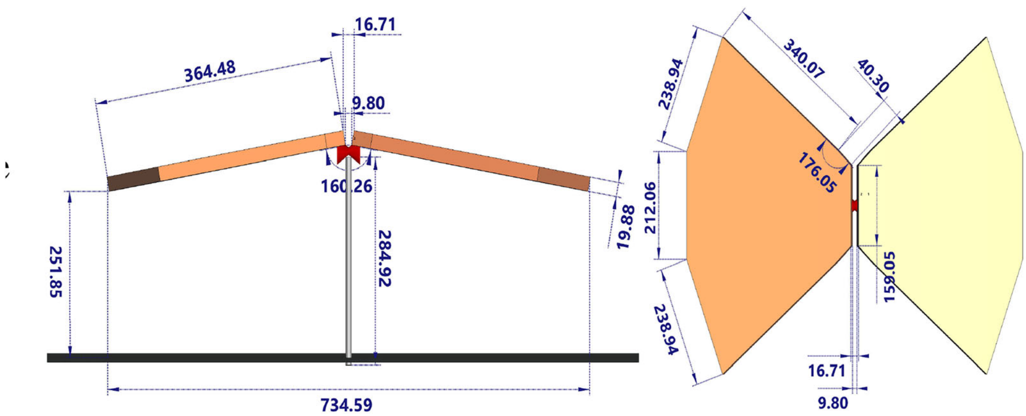

Figure 3. (Left) Front view and (right) top view of the 120–360 MHz antenna placed over the reflector along with the dimensions.

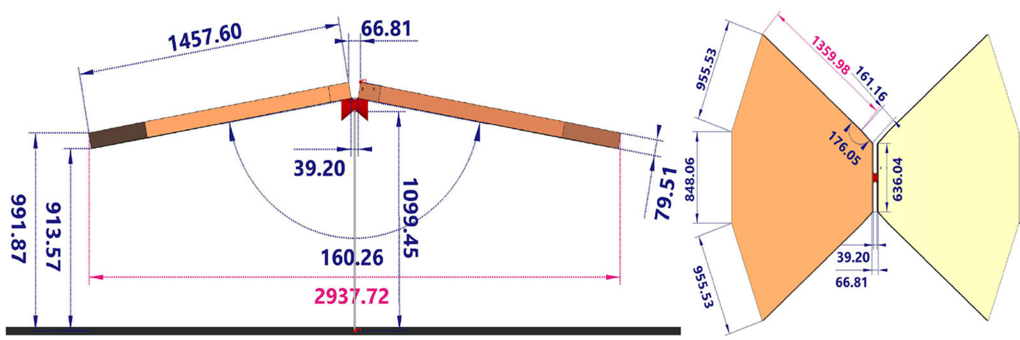

Figure 4. (Left) Front view and (right) top view of the 30–90 MHz antenna placed over the reflector along with the dimensions.

two arms of the dipole are placed over an electromagnetically transparent blue styrofoam maintaining the optimized gap and tilt angle between them. The balanced output of the dipole antenna is connected using a pair of copper strips to the primary input of the transformer-based balun housed inside an enclosure made of polyvinyl chloride (PVC) material. The single-ended output of the transformer is brought down to the antenna base through an air–core coaxial cable. The balun along with the coaxial cable is anchored rigidly to a nonmetallic stand kept at the center of the antenna. The fabricated structures of 30–90 MHz antenna and 120–360 MHz antenna are shown in figure 5. The balun connected to the coaxial cable and the stand is shown in figure 6. Also shown is the balun mounted on FR4 printed circuit board (PCB) laminate with its input and output connected to the copper strips and SubMiniature version A (SMA) connector, respectively. The balun box is designed in such a way that the inputs are brought out sideways with the top lid closed. This design prevents water from top entering directly into the box.

Table 1. Optimized values of various structural and electrical parameters of 30–90 and 120–360 MHz antennas

Sl. No.	Parameter	30–90 MHz antenna	120–360 MHz antenna
1.	Length of each arm	1457.6 mm	364.48 mm
2.	Thckness ofarm	79.5 mm	19.88 mm
3.	Gap between arms (top side/bottom side)	66.8 mm /39.2 mm	16.7 mm /9.8 mm
4.	Height of phase center above reflector	1139.2 mm	284.9 mm
5.	Tilt of each arm	+10 deg	+10 deg
6.	Reflector dimension	16 m × 16 m	4 m × 4 m
7.	Design frequency	56.6 MHz	226.5 MHz

Figure 5. Fabricated structure of (left) 30–90 MHz antenna and (right) 120–360 MHz antenna placed on an electromagnetically transparent stand made of blue styrofoam material.

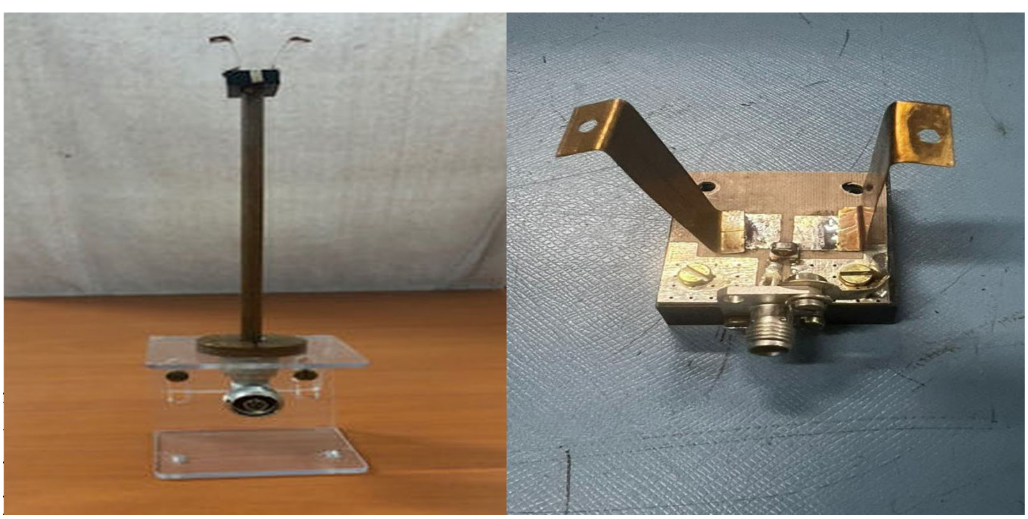

Figure 6. (Left) Photograph showing the balun box placed at the top of an air–core coaxial transmission line. A pair of copper strips is brought out of balun to get connected to the antenna. The output of the balun is connected to the center conductor of the air–core coaxial line, which is anchored to a c clamp made out of acrylic material. (Right) Balun TC1-1-13MG2+ mounted on an FR4 PCB laminate is shown with its input connected to two copper strips and the output to the SMA connector.

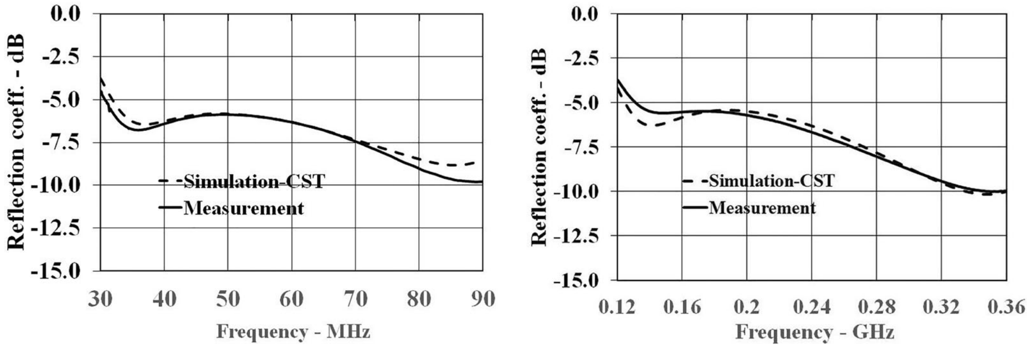

Figure 7. Reflection coefficient of (left) 30–90 MHz antenna and (right) 120–360 MHz. The solid line represents the measurement, and the dotted line represents the simulation.

Figure 8. Experimental setup for the measurement of the radiation pattern of the 120–360 MHz antenna. The 120–360 MHz antenna (AUT) is kept along east–west direction on a 4 m × 4 m metal reflector. A standard dipole antenna from ETS-Lindgren is used as a transmitter fixed to a movable stand at a height of 2 m above the reflector. During the measurement, it is moved horizontally to different distances from AUT.

5. Measurement of reflection coefficient

The antenna is a transducer that is used primarily to convert electromagnetic energy propagating in space into an electric current and vice versa. This is based on the principle of electromagnetic induction. The current induced in the antenna during reception via coupling is governed mainly by the impedance mismatch between the free space and the antenna and the antenna and the transmission line connected at its output terminals. The allowed impedance mismatch and its variation across frequencies are application-dependent.

While designing the antennas for low-frequency applications in radio astronomy and observational cosmology, two important requirements were considered: i) wide bandwidth (more than an octave), ii) smooth spectral response, and iii) frequency-independent radiation and impedance response. In radio astronomy, simultaneous observation of the sky at multiple frequencies is highly desired to have a complete understanding of the celestial source, which has unique information about itself at different frequencies. Smooth spectral response is another important requirement in wideband sky observation for effectively performing the bandpass calibration. The frequency-independent response makes the spectral response feature-free, which may mimic the nature of the

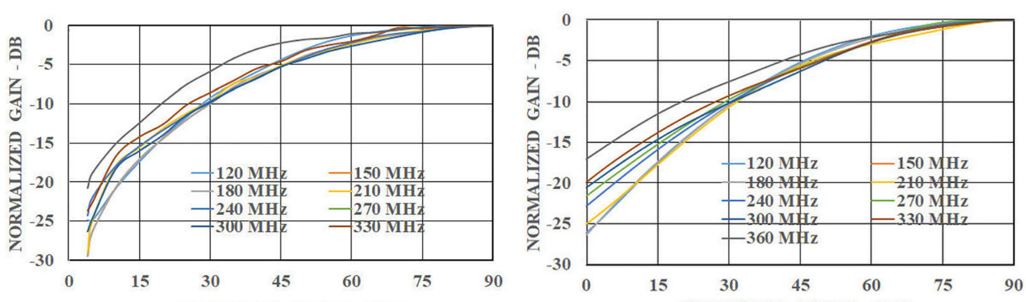

Figure 9. Radiation patterns (left) measured and (right) simulated of the 120–360 MHz antenna.

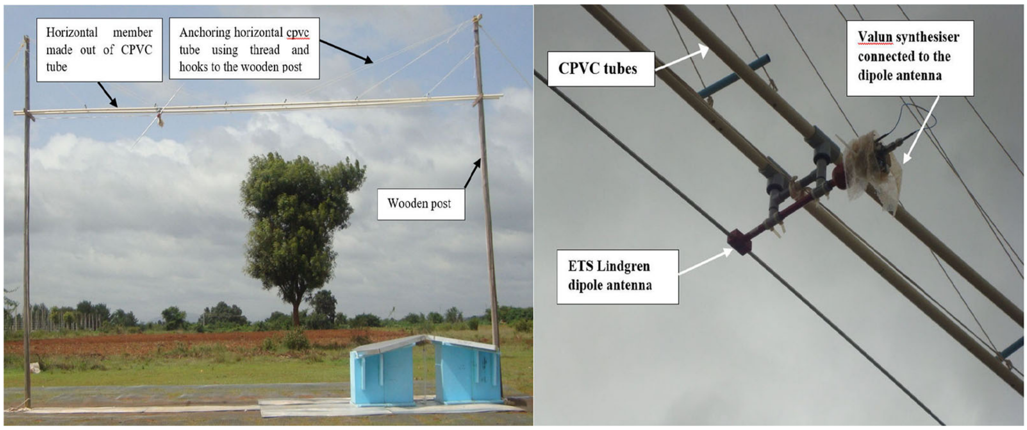

Figure 10. (Left) Fabricated structure of the experimental setup used for measuring the radiation pattern of the 30–90 MHz antenna. A standard dipole antenna from ETS-Lindgren used as a transmitter is moved horizontally on a pair of CPVC tubes. (Right) The CPVC tubes shown glide standard dipole antenna horizontally. The standard dipole antenna is rigidly fixed to the CPVC structure using a T and collar arrangement. A Valon synthesizer is used to feed continuous wave (CW) signal to the standard dipole antenna for transmission.

cosmological signal confusing the detection process. To meet these requirements, the structural parameters of the antenna were optimized. In the process, the reflection coefficient was treated as a free parameter and it was ensured that it would have a modest value of about -4 dB at the lowest frequency in the band of 30–90 MHz. This can be accepted based on the fact that i) the sky is bright at low frequencies ($<$ 150 MHz) and having a poor reflection coefficient may have less effect on the signal loss and ii) for cosmological experiments like the epoch of recombination [11], as the signal is over the entire sky, less coupling of it by the antenna may be compensated by observing the sky over a longer period of time. At high frequencies ($>$ 150 MHz), the antenna does suffer from signal loss. Thus, 120–360 MHz antenna will be less efficient. However, due to its large bandwidth, it can be used with 30–90 MHz antenna during simultaneous sky observation. The amount of sky signal lost while getting coupled to the receiver electronics through the antenna is indicated by the reflection coefficient parameter of the antenna.

The reflection coefficient was measured using Keysight's N9912A FieldFox handheld radio frequency (RF) analyzer. The measurement was made in a field that was free from objects that would reflect signals radiated by the antenna, thus corrupting the reflection coefficient measurement of the latter. A 4-m $\times$ 4-m square mesh of 1-inch-by-1-inch hole size was used as the reflector for the 120–360 MHz antenna. A similar mesh of 16 m $\times$ 16 m size was used for 30–90 MHz antenna. A coaxial cable of the smallest length was used to connect the antenna to the network analyzer

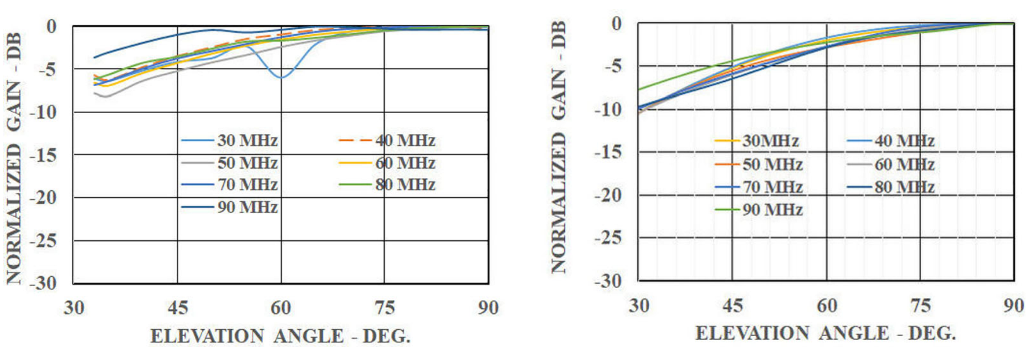

Figure 11. Radiation patterns (left) measured and (right) simulated of the 30–90 MHz antenna. The patterns were measured at 30, 40, 50, 60, 70, 80, and 90 MHz. The minimum elevation angle is restricted to 33 deg due to the constraint imposed by the measurement setup.

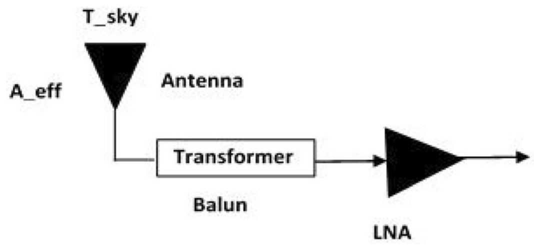

Figure 12. Antenna connected to the transformer (balun) and LNA.

while making the measurement. After calibrating the instrument along with the connecting cable, the reflection coefficients of both antennas were measured and plotted along with the simulation results as shown in figure 7. The measurements match closely with the simulation results and have a spectral response without undesirable sharp features. It is observed that both antennas have similar impedance characteristics as expected as each one of them is a scaled version of the other.

6. Measurement of the radiation pattern

The radiation pattern is a fundamental parameter of an antenna indicating its sensitivity to the sky signal as a function of angle in the sky. It is measured at every 10 MHz in the 30–90 MHz band and at 120, 150, 180, 210, 240, 270, 300, and 330 MHz in the 120–360 MHz band. While measuring the radiation pattern, the 120–360 MHz antenna (antenna under test (AUT)) was kept at the center of a 4 × 4-sq.-m aluminum sheet along east–west direction. A tunable dipole antenna from ETS-Lindgren was used as a transmitter for transmitting signal toward AUT maintaining the same polarization. It was kept at a height of about 2 m above the reflector on a moveable stand as shown in figure 8. An AnaPico signal generator was used to feed the signal to the transmitter at different frequencies. The signal received by AUT was measured using N9912A RF analyzer.

While making the measurement of the antenna gain at different elevation angles, the transmitter was moved to different distances from the AUT as determined by the elevation angle and tilted appropriately to have its maximum gain directed towards the phase center of the AUT. In each position, signals of different frequencies were fed to the transmitter and the received signal by AUT was measured using the RF analyzer. For the 120–360 MHz antenna, the E-plane pattern measurements were made for the elevation angle covering the range of 5 to 90 deg at all frequencies mentioned earlier. The patterns measured are plotted along with the simulation results in the figure 9. It is observed that the measured patterns match very closely with the simulation. The ripples observed are attributed to reflections in the connecting cables used in the measurement setup.

Similarly, the E-plane radiation pattern measurement was also carried out for the 30–90 MHz antenna. As this was a low-frequency antenna, the measurement setup was required to be large because of the large wavelength involved. Measurement at low frequencies is a big challenge because of i) the large setup involved and ii) the presence of multiple reflections from objects surrounding the antenna. To minimize the effect of multiple reflections, a clean and large volume of space free from stray wires and other metallic objects was ensured around the antenna as they offer a large cross section for the low-frequency signal for the reflection.

The setup used for the measurement of the radiation pattern in the frequency range of 30–90 MHz is shown in figure 10. The 30–90 MHz antenna (AUT) supported by an electromagnetically transparent styrofoam material was kept on a 16 m × 16 m reflector made of galvanized mesh of 1-inch-by-1-inch square hole. A standard dipole antenna from ETS-Lindgren was used as a transmitter and was placed at a height of 18 ft (≈ far-field distance of the AUT at 100 MHz) from the phase center of the AUT. The standard dipole antenna was laterally moved over a pair of chlorinated PVC (CPVC) tubes laid horizontally and supported on either side by two vertical wooden pillars grouted firmly on the ground. The horizontal movement of the transmitter was controlled from the ground by pulling a string attached to it. The sagging of CPVC tubes was minimized by pulling them vertically with several nylon wires tied to them using hooks at different locations along their length. The nylon wires were pulled taut and secured at the vertical wooden pillars. Using the T and collar arrangement, the transmitter was moved along the tubes. Tilting of the transmitter toward AUT for directing its maximum gain toward it was accomplished by manually rotating it to the required angle. The lateral movement of the transmitter from AUT was restricted to 30 ft. beyond which, due to the sagging effect, the tubes could not be held horizontally. This limited the lowest elevation angle at which antenna gain could be measured to 33 deg above the horizon. Because of this, the radiation pattern could be measured only in the elevation angle range of 33–90 deg. A Valon 5009a, a dual-frequency synthesizer module capable of producing signals in the frequency range of 23 to 6000 MHz, was connected to the transmitter for transmitting them toward AUT. The power of the signal received by AUT was measured using the RF analyzer.

Using the setup described above, the radiation patterns were measured and plotted along with simulation results as shown in figure 11. The measured patterns show a similar trend as the expectation at most of the frequencies. The results obtained indicate that the experimental setup devised can be used to make pattern measurements at low frequencies, which often pose challenges due to the large wavelength involved. The dip observed in the pattern at 30 MHz is attributed to the reflection from the nearby structural member in the measurement setup.

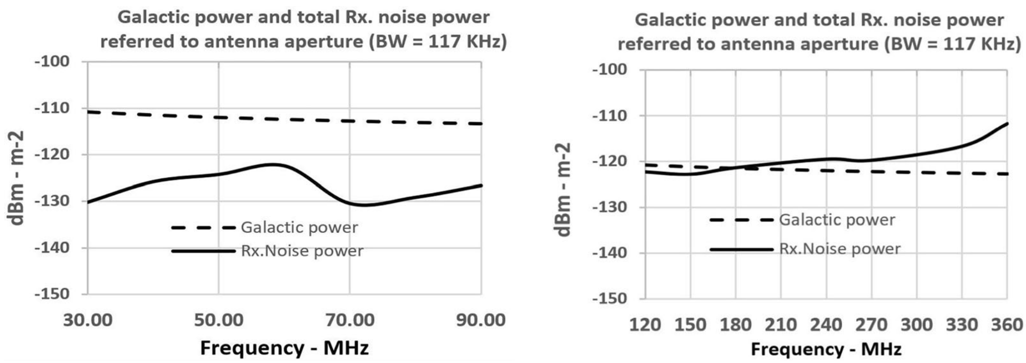

Figure 13. Sensitivity of 30–90 MHz and 120–360 MHz antennas.

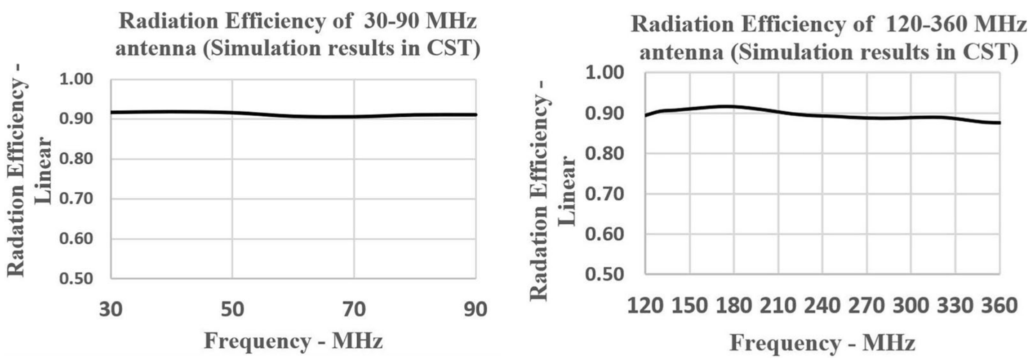

Figure 14. Radiation efficiency of 30–90 MHz and 120–360 MHz antennas.

The E-plane radiation patterns of both 120–360 MHz and 30-90 MHz antennas are found to be frequency-independent with about 10% deviation in their half-power beamwidths across their operating bands. The 120–360 MHz antenna is observed to have a gain toward the horizon 20 dB less than its gain at the zenith, thus exhibiting less sensitivity to the man-made RF interference (RFI) coming from that direction. We anticipate similar behavior for the 30–90 MHz antenna as that of the 120–360 MHz antenna as the former is the scaled version of the latter.

7. Sensitivity of antenna

The sensitivity of an antenna is in general the minimum signal power that it can detect. For a lossless antenna, the sensitivity is limited primarily by the noise generated by sources external to it such as ohmic loss, low-noise amplifier (LNA), and sky background [12]. We compute the sensitivity of antennas operating in the frequency ranges of 30–90 MHz and 120–360 MHz with the receiver system connected to it as shown in figure 12. The balanced outputs

Table 2. Comparison of the performance characteristics of various wideband antennas.

Sl. no.	Antenna type	Structural bandwidth	Operating bandwidth	Polarization	Reflection coefficient	Radiation pattern
1.	MWA	80–300 MHz	30.72 MHz [15]	Dual linear	-3 to -9.5 dB nonsmooth spectral response [16]	Frequency dependent
2.	SKA	50–350 MHz	50–350 MHz	Dual linear	-3 to -12 dB nonsmooth spectral response [6]	Frequency dependent
3.	LFRT	30–90 MHz 120–360 MHz 270–360 MHz	30–90 MHz 120–360 MHz 270–360 MHz	Single linear	−4 to −8 dB smooth spectral response	Frequency independent

of the antennas are passed through a transformer-based balun for converting them to a single-ended mode before feeding them to the LNA. The balun has a loss of about 1 dB constant over the entire band of antennas, and LNA has a noise temperature T_{LNA} of about 63 K over the frequency range of 30–90 MHz and 90–120 K over 120–360 MHz band. The net receiver noise is contributed by both LNA and noise due to ohmic loss (T_{loss}). Along with the receiver noise, the noise due to the sky and ground also add up to constitute the total system noise, which will be used to calculate the minimum detectable signal by the radio receiver.

The sky noise is generally contributed by i) man-made RFI and ii) background noise in the sky. The man-made interference depending upon its strength will either corrupt the entire spectrum of the sky signal measured during the astronomical observation by saturating the receiver electronics or affect certain frequency channels. It also plays a dominant role in cosmological experiments, which aim at detecting very faint signal for probing the physical processes during the evolution of the Universe. Therefore, it becomes imperative to select a site that is free from RFI for conducting the sensitive experiments. In the absence of any man-made RFI, the background noise in the sky will be primarily due to our local galaxy, which is observed to have different effects in different frequency ranges. Below 200 MHz, it is found to dominate the total system noise power. However, above this frequency, it is found to have less power than the receiver noise.

The method of determining the sensitivity of antenna involves computing the noise power of all the sources present at the aperture of the antenna. The sky noise power contributed mainly by the galactic foreground in the absence of strong RFI is calculated based on the formulation given in [13] for the frequency range of 30–90 MHz and [14] for the frequency range of 120–360 MHz over 117 KHz bandwidth (spectral resolution of the digital receiver used) and 2π steradian. The thermal noise power from the LNA and the ohmic loss calculated from their respective temperatures are referred to the antenna aperture by appropriately dividing them by the transmission coefficients of the antenna and balun and the effective area of the antenna to enable them compare with the galactic noise power incident.

The plots in the figure 13 show the noise power contributions from both the sky (Galactic) and the receiver in both bands. The sky power is observed to be dominant in the 30–90 MHz band limiting the minimum detectable power to about -110 to -112 dBm on average. In the band of 120–360 MHz, the receiver noise power starts dominating the sky power from about 200 MHz in the band. The minimum detectable power starts from -120 dBm at 120 MHz and extends to -110 dBm at 360 MHz.

In radio astronomy, the total noise power is generally expressed in terms of system temperature (T_{sys}). Similarly, the minimum detectable power is also expressed as the minimum detectable temperature. It is related to the system temperature, bandwidth, and time of integration (τ) through the relationship given by

$$Minimum\ \ detectable\ \ temperature = \frac{T_{sys}}{\sqrt{B\tau}}. \tag{1}$$

The minimum detectable temperature could be reduced by increasing the measurement bandwidth (B) and the time of integration τ of the signal. The variation of the thermal noise of the ground with frequency is dependent on the frequency response of the radio receiver. Similarly, LNA noise is transistor-dependent and the sky noise primarily from the (Galaxy) varies with a temperature spectral index of $\approx$ -2.44. Based on the cumulative effect of each of the above noise components as a function of frequency, the minimum detectable temperature of the measuring radio receiver will be determined.

8. Radiation efficiency analysis

The radiation efficiency is one of the important performance indicators of an antenna. It indicates how efficiently the antenna converts the RF signal accepted at its input terminals into the radiation. If the antenna is lossy, some portion of the power accepted at the input terminals gets dissipated in the form of heat and the rest gets radiated. This results in a radiation efficiency of less than 100%. Thus, the radiation efficiency can be written in the form of an equation as

$$Radiation\ \ efficiency(\eta) = \frac{Power\ Radiated}{Power\ accepted} \tag{2}$$

where power radiated P_{rad} =

$$\int_0^{2\pi}\int_0^{\frac{\pi}{2}} U d\Omega \tag{3}$$

where U is the radiation intensity (W Sr^{-1}) and Ω is solid angle of the antenna (steradian).

In the antennas designed by us, the balun used to convert the balanced output of the antenna to unbalanced output has a loss of about 1 dB. This was incorporated in the CST microwave electromagnetic simulation software, which was used to design and optimize the antenna structural parameters. The radiation efficiencies of the optimized structure were computed in both 30–90 MHz and 120–360 MHz bands as shown in the figure 14. The antennas are found to have radiation efficiencies in both bands in the range of 0.91 to 0.92.

9. Comparison of performance of antenna designed with other existing wideband antennas

The table 2 compares the performance characteristics of different wideband antennas existing with the antenna designed by us with regard to bandwidth, reflection coefficient, and radiation patterns. The antennas designed by us in the frequency bands of 30–90 MHz and 120–360 MHz are found to be frequency-independent with about 10% deviation in their half-power beamwidths across their respective operating bands.

10. Summary

For the LFRT, we have designed and developed two reflector-based planar, sinusoidally profiled, and tilted dipole antennas having 1:3 bandwidth to cover the frequency bands of 30–90 MHz and 120–360 MHz. The antennas have been structurally optimized to have i) a moderate reflection coefficient of less than −4 dB over their operating bands with a smooth spectral response and ii) frequency-independent E-plane radiation patterns with a maximum dispersion in their half-power beamwidths of about 10% across their operating bands. The frequency-independent characteristic is expected to ease the calibration of the bandpass response of the antenna. The antennas designed will be used to probe the sky at longer wavelengths for the detection of transients and measurement of broadband polarization, both steady and transient, of a wide variety of sources including pulsars.

Acknowledgements

We acknowledge help from the staff of the Electronics Engineering Group of the Raman Research Institute who helped us in various stages of testing of antennas. We also thank the staff of the mechanical engineering services for fabricating the antennas and making the required supporting structures out of styrofoam material. The members of the Gauribidanur Observatory were involved in the field measurement of the antennas. Help from Mr. Anand and Mr. Venugopal of Gauribidanur observatory are acknowledged for their ideas in implementing the setup for the measurement of the radiation pattern of the 30–90 MHz antenna.

References

[1] Rao K B R, Nagaraja H N and Deshpande A A 2021 A Wide-Band RF Receiver system for Sky Watch Array Network, Technical report (Link: *http://dspace.rri.res.in/handle/2289/7842*), Raman Research Institute, Bengaluru

[2] Di Ninni P, Bolli P, Paonessa F, Pupillo G, Virone G and Wijnholds S J 2020 Comparison Between Measured and Simulated Antenna Patterns for a LOFAR LBA Array, in: 14^{th} European Conference on Antennas and Propagation (EuCAP), 1–5

[3] Singh K, Bähren L, Buitink S, Falcke H, Hörandel J, Horneffer A and Scholten O 2009 Ultra-High Energy Cosmic Ray and Neutrino Detection with LOFAR, in: Proceedings of the 31^{st} ICRC

[4] Ellingson S W, Taylor G B, Craig J, Hartman J, Dowell J, Wolfe C N, Clarke T E, Hicks B C, Kassim N E, Ray P S, Rickard L J, Schinzel F K and Weiler K W 2013 The LWA1 radio telescope. *IEEE Transactions on Antennas and Propagation* 61: 2540–2549

[5] Lonsdale C J, Cappallo R J, Morales M F, Briggs F H, Benkevitch L, Bowman J D, Bunton J D, Burns S, Corey B E, DeSouza L and Doeleman S S 2009 The Murchison Widefield Array: Design Overview. *Proceedings of the IEEE* 97(8): 1497–1506

[6] Bolli P, Mezzadrelli L, Monari J, Perini F, Tibaldi A, Virone G, Bercigli M, Ciorba L, Di Ninni P, Labate M G and Loi V G 2020 Test-Driven Design of an Active Dual-Polarized Log-Periodic Antenna for the Square Kilometre Array, in :*IEEE Open Journal of Antennas and Propagation*, 1, 253–263

[7] Kavitha K, Raghunathan A, Somashekar R, Girish B S, Srivani K S, Subrahmanyan R, Udaya Shankar N, Sathyanarayana Rao M, Singh S and Nambissan J 2021 Wideband antenna for detecting global signal from the recombination epoch, in: *IEEE Indian Conference on Antennas and Propagation(InCAP)*, 367–370

[8] Agaram R, Sethi S, Deshpande A A, Raghavendra K B, Satish K, Arasi S, Vinod K R, Nagaraj H N, Srivani K S, Girish B S and Kavitha K 2023 A Wideband Single Polarization Radio Receiver – Precursor to Low Frequency Radio Telescope, in: *International Conference on Computer, Electronics and Electrical Engineering and their Applications (IC2E3)*, 1–6

[9] WIPL-D d.o.o. Wipl-d pro description. Available online: https://wipl-d.com/products/wipl-d-pro/

[10] CST Studio Suite, "*CST Microwave Studio*", 2023

[11] Raghunathan A, Subrahmanyan R, Shankar N U, Singh S, Nambissan J, Kavitha K, Mahesh N, Somashekar R, Sindhu G, Girish B S and Srivani K S 2021 A floating octave bandwidth cone-disk antenna for detection of cosmic dawn. *IEEE Transactions on Antennas and Propagation* 69(10): 6209–6217

[12] Ellingson S W and Kramer T C 2005 Sensitivity and bandwidth of low-gain active antennas below 100 MHz. *IEEE Antennas and Propagation Society International Symposium, Washington, DC, USA* 3A: 561–564

[13] Spinelli M, Bernardi G, Garsden H, Greenhill L J, Fialkov A, Dowell J and Price D C 2021 Spectral index of the Galactic foreground emission in the 50–87 MHz range. *Monthly Notices of the Royal Astronomical Society* 505(2): 1575–1588

[14] Haslam C G T, Salter C J, Stoffel H and Wilson W 1982 A 408 MHz all-sky continuum survey. II-The atlas of contour maps, in: *Astronomy and Astrophysics Supplement Series*, Vol. 47, Jan., p. 1, 2, 4–51, 53–142., 47, 1

[15] Tingay S J, Goeke R, Bowman J D, Emrich D, Ord S M, Mitchell D A, Morales M F, Booler T, Crosse B, Wayth R B and Lonsdale C J 2013 The Murchison widefield array: the square kilometre array precursor at low radio frequencies, in: *Publications of the Astronomical Society of Australia*, 30, e007

[16] Mani H and Bowmann J 2010 MWA Antenna Impedance Measurements (Link:*http:// loco.lab.asu.edu/ loco-memos / loco002.pdf*)